Journal of Polymers and the Environment (2023) 31:3418–3432
https://doi.org/10.1007/s10924-023-02790-5

ORIGINAL PAPER

Adsorption of BSA Protein in Aqueous Medium Using Vegetable Tannin Resin from *Acacia mearnsii* (Mimosa) and Modified Lignocellulosic Fibers from the Bark of *Eucalyptus citriodora*

Dalvani S. Duarte[1] · Francisco H. M. Luzardo[1] · Fermin G. Velasco[1] · Ohana N. de Almeida[1] · Guisela D. R. Z. Bedon[1] · Glauber G. Nascimento[1] · Thais B. V. Andrade[1] · Luiz C. Salay[1]

Accepted: 7 February 2023 / Published online: 16 March 2023

Abstract

Proteins are abundant biomolecules found in human cells, as well as pathogenic bacteria and viruses. Some of them become pollutants when released into water. Adsorption is an advantageous method for separating proteins in aqueous media since proteins are already immobilized on solid surfaces. Adsorbents with surfaces rich in tannins are efficient due to their affinity for strong interactions with the various amino acids that make up proteins. This work aimed to develop an adsorbent for protein adsorption in aqueous medium using lignocellulosic materials modified from eucalyptus bark and vegetable tannins. A more efficient resin was prepared containing 10% eucalyptus bark fibers and 90% tannin mimosa by condensation with formaldehyde, and it was characterized by UV–Vis, FTIR-ATR spectroscopy and determinations of degree of swelling, bulk and bulk density and specific mass. For UV–Vis spectroscopy the percentage of condensed and hydrolysable tannins in the extracts of fibers of the dry husks of Eucalyptus Citriodora was estimated and it was also determined your soluble solids. The study of bovine serum albumin (BSA) adsorption was carried out in batch with quantification by UV–Vis spectroscopy. The most efficient prepared resin obtained $71.6 \pm 2.78\%$ removal in a solution of 260 mg L^{-1} of BSA working in a better pH range of the aqueous solution of BSA in its isoelectric point, ~ 5, 32 ± 0.02, under these conditions, the synthesized resin can reach a maximum BSA adsorption capacity of $\sim 26.7 \pm 0.29$ mg g^{-1} in 7 min. The new synthesized resin presents good prospects for adsorption of proteins or species that in their structure have higher percentages of amino functional groups or amino acids with aliphatic, acidic and/or basic hydrophilic characteristics.

✉ Luiz C. Salay
lcsalay@uesc.br

[1] Department of Exact e Technological Sciences, State University of Santa Cruz – UESC, Ilhéus, Bahia, Brazil

Graphical Abstract

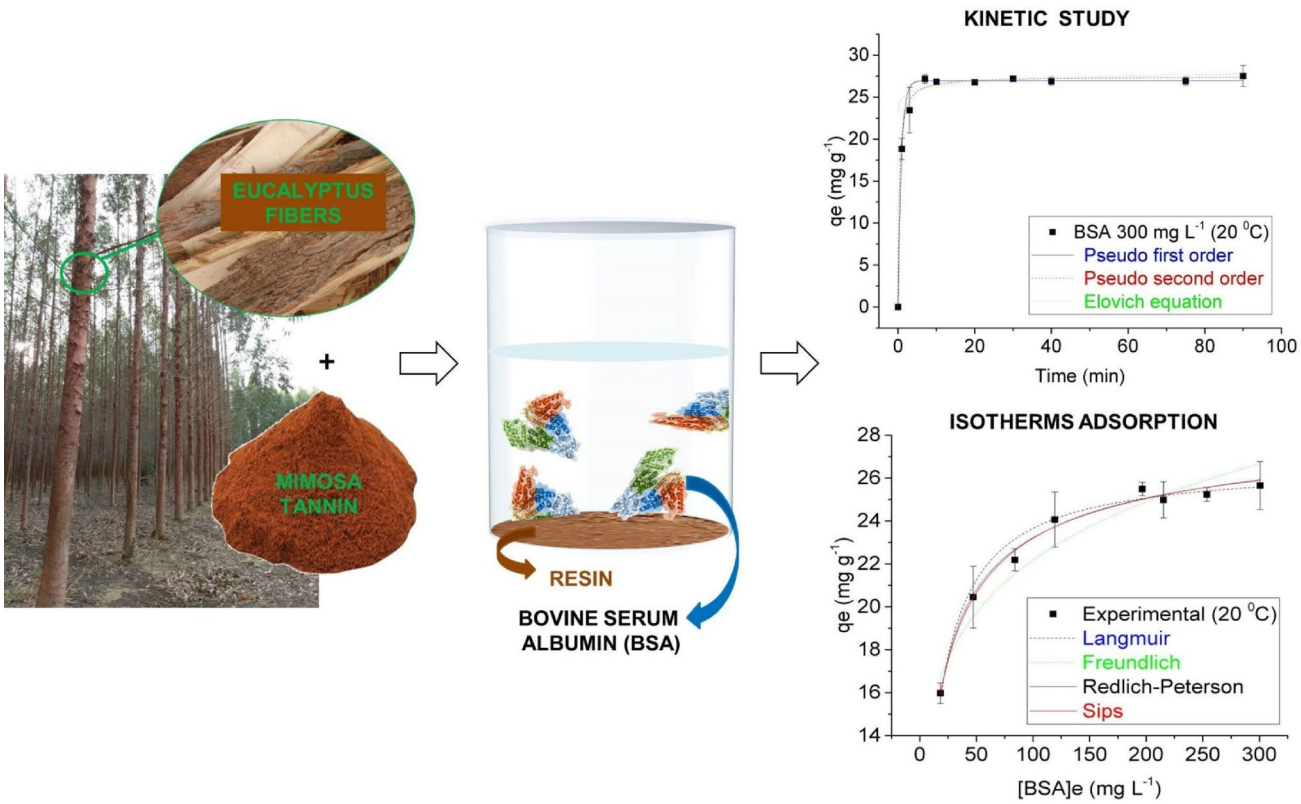

Keywords Water pollution · Protein adsorption · FTIR-ATR spectroscopy · Tannin resin · Lignocellulosic fibers · UV–Vis spectroscopy

Introduction

The immobilization of biomolecules on solid surfaces is important in several areas, such as biomedicine, biotechnology and environmental sciences. Several biomolecules have been immobilized on surfaces, such as polysaccharides [1], nucleic acids [2], lipids [3, 4], proteins and peptides [5, 6]. Proteins require attention because they are abundant, found in animal and plant sources, and have broad biological functions, such as structural and regulatory [6]. Given the abundance and applicability of proteins, controlling the disposal of this biopolymer is important, as they become polluting organic matter when released into affluents and effluents [7].

Proteins make up vital structures, such as human cells, as well as pathogenic bacteria and viruses, these have an external protective envelope formed by proteins and lipids and are present in different environments, such as water [8]. Viruses such as astroviruses, rotaviruses and the SARS-CoV causing the COVID-19 pandemic are already detected in hospital, domestic and general urban effluents and the adsorption focused on the external protein characteristics of the viruses is identified as a way of elimination and/or concentration of them from aquatic environments [9]. Conventional treatment with the application of chlorinated disinfectants is capable of inactivating viruses and bacteria, but their protein residues remain in the environment and the infection or restructuring capacities are still unknown, so the use of effluent water without a complete and effective treatment is a potential generator of risk to human, animal and environmental health [10].

Proteins are released into effluents from industrial processes and science already points to possibilities for their recovery and/or fluid decontamination. Yadav and collaborators [7] presented a work that proposes the recovery of microbial proteins resulting from the polyhydroxyalkanoate (PHA) production process as a way to boost this trade, Kurup et al. [11] recovered 96% of lipids and 46% of proteins, mainly casein, from the sewage of a dairy plant applying sodium lignosulphonate as a low-cost coagulant. Bethi and collaborators [12] recovered proteins by precipitation from fish, cattle, poultry and goat slaughterhouse wastewater. Blood proteins were the majority

(albumins and globulins) with higher levels of essential amino acids, mainly leucine. These recycled products become raw material for animal feed, adhesive materials, bioplastics manufacturing, among others. Hwang and collaborators [13] applied solubilization, ultrasonication and alkaline treatment to recover proteins from domestic sewage sludge, BSA was used as a standard for protein characterization and quantification and the protein isolate showed potential for animal feed.

Commonly reported methods for recovering proteins in aqueous media are physical, chemical and biological sometimes associated. According to Li and collaborators [14], Coglitore [6] and Latour [15] adsorption is presented as an advantageous method compared to traditional methods used for protein separation. This method reduces steps, reagents and energy consumption, as the adsorbent-adsorbate interaction is mainly dependent on the affinity between the species, their active functional groups, temperature, contact surface, isoelectric point and pH.

The adsorbent surfaces developed for proteins are commonly based on self-assembly of nanostructures, polymeric grafts, use of metallic nanoparticles, varied material functionalization techniques employing different reagents and sophisticated technologies [6]. These examples report positive responses, but increase the cost of product synthesis and application. Tannic species have been used to add protein adsorbent capacity, usually they are synthetic polymers or inorganic materials that form bonds strong enough to make the tannins insoluble, as Bazzaz and collaborators [16] who synthesized and modified hexagonal mesoporous silica by applying tannic acid and amine for the adsorption of bovine serum albumin (BSA) from aqueous media. The strong affinity of vegetable tannins for proteins is known. They react by complexation and/or coagulation, characteristics used for a long time, for example, for the identification of these species in solutions and in animal skin tannery, being especially associated with condensed tannins [17].

Tannic polyphenols can be classified into three classes according to their chemical structures, hydrolysable, condensed and complex oligomeric [18]. Condensed tannins are oligomeric flavonoids capable of undergoing polycondensation. Flavonoids are a diversity of metabolite groups based on a phenylalanine-derived heterocyclic ring system called the B ring and polyketide biosynthesis called the A ring [18]. The fundamental structural unit of the flavonoid group is the phenolic core of flavan-3-ol (catechin) [17]. The possible variations to this monoflavonoid derive from the different possible combinations for each ring A and B, in detriment to the amount and disposition of the phenolic hydroxyls. Condensed tannins can be reclassified according to the A-ring structure, therefore, subdividing into phloroglucinolics, which have two hydroxyls in this ring, or resorcinolics with a single hydroxyl group in the A-ring [19].

Tannins are commercially searched and have already been identified in species of great national and world production, such as eucalyptus, with its residual biomass (bark) composed mostly of lignin, cellulose and hemicellulose, as well as highly active phenolic polyhydroxy compounds [20, 21]. The commercial mimosa tannin of Acacia mearnsii is scientifically explored and its characterization points to a complex mixture of resorcinolics and phloroglucinolics rich in condensed structures [22]. The interaction of mimosa tannin with proteins has already been confirmed, as in the recent study by Pizzi (2021) [23] using collagen in order to elucidate the nature of the interactions of these species in aqueous media, confirming strong covalent bonds.

The literature presents consolidated research on the use of lignocellulosic materials [24] and tannins that have undergone physical and chemical modifications resulting in low-cost adsorbents with increased efficiency for the treatment of metal contamination in water [20, 25]. Similarly, the polymerization of lignocellulosic fiber components through polycondensation reactions of polyphenols such as vegetable tannins has already been developed [26]. This technique has also been used to enrich plant fibers with tannin extracts and other components, generating functionalized resins [27, 28]. However, these or similar products had not been studied to generate adsorbents for protein adsorbates. The exploration of the characteristics of products of plant origin are not at the same level of development for the adsorption of different inorganic and organic materials.

The strength of the protein-tannin interaction is known and used for innovations, for example in the manufacture of fully biologically sourced wood adhesives via a covalent reaction between soy protein isolate and commercial quebracho flavonoid tannin [29]. BSA is the model protein studied in this work, it is composed of several amino acids: 34.63% by the aliphatic amino acid group, 16.99% by acidic hydrophilic, 16.99% by basic hydrophilic, 16.29% by neutral hydrophilic, 8.4% by aromatic and 6.7% by those that contain sulfur [30]. In a theoretical study Hernández [31] concluded that the acidic and basic hydrophilic amino acids and the aliphatic amino acid leucine form stable complexes against condensed tannins. Recently, it was concluded that protein molecules interact with different active sites on the adsorbent surface, spreading to the maximum interaction in empty spaces [15]. Due to the large amount and diversity of amino acids that make up BSA, it presents possibilities of diverse interactions with a surface rich in condensed tannins.

In a recent work [32] it was concluded that with pure or modified tannins the elaboration of new materials is in full development and that there are properties to be explored. In this sense, the examples of applications together with the characteristics of vegetable tannins and lignocellulosic materials make them renewable raw materials, with chemical qualities capable of generating adsorbents with potential

use to separate proteins in an aqueous medium. The present work aimed to develop an adsorbent for the adsorption of BSA in aqueous medium using lignocellulosic materials modified from the bark of *Eucalyptus citriodora* and vegetable tannins from *Acacia mearnsii* (Mimosa).

Materials and Methods

Collection and Pre-treatment of Eucalyptus Bark

The bark of *Eucalyptus citriodora* was collected from woody tree harvest residues. They were washed in deionized running water, cut into 2–3 cm pieces, dried in a solar oven for 48 h and in an electric oven (100 ± 2 °C) until mass was not variable, then they were crushed in a Wiley knife mill and selected in a mesh sieve with a particle size between 20 and 150 mesh.

Obtaining Extractives of *Eucalyptus citriodora* Bark Fibers

The extraction was aqueous, hot and in a closed reactor with liquid phase recirculation, thus, 2 g of the ground eucalyptus fibers received 250 mL of deionized water and were subjected to extraction in a Soxhlet at a temperature of 90 ± 3 °C for 2h30min. The extract was cooled to room temperature (20 ± 1 °C), transferred to a 250 mL volumetric flask and filled with deionized water.

Determination of Total Soluble Solids (TSS)

To determine the total soluble solids (TSS) extracted, three samples of 25 mL of the aqueous extract of eucalyptus fibers ground in beakers with previously measured masses were placed, and these were subjected to drying in an oven (at 103 ± 2 °C) until constant weight. The average mass of the samples corrected by the standard deviation was the parameter to measure the total mass of solids dissolved in the 250 mL solution of the extract. In sequence, this total mass was the parameter for calculating the TSS percentage of the sample of 2 g of dry and crushed eucalyptus bark used. UV–Vis Spectroscopy.

All UV–Vis spectroscopy experiments were performed using 10 mm quartz cuvettes in the SP-220 BIOSPECTRO digital spectrophotometer operating between 200 and 1000 nm.

Calibration Curves for Tannic Compounds

The species used for tannin quantification were tannic acid (TA) 88% (ALPHATEC) and gallic acid (GA) anhydrous 98.0% (VETEC). All were prepared as aqueous solutions in deionized water from concentrated stock solutions of 100 mg L^{-1} for TA and 20 mg L^{-1} for GA. Subsequently, the different concentrations of each solution were prepared by dilution to 10.0 mL in a volumetric flask, for TA there were 10 concentrations of 10–100 mg L^{-1} and for GA 8 concentrations between 4 and 18 mg L^{-1}. Absorption quantifications were made at wavelengths of 280 nm for TA and 265 for GA.

BSA Protein Calibration Curve

The protein used in the adsorption tests was 96% lyophilized bovine serum albumin (BSA) (SIGMA). A concentrated solution in deionized water of 600 mg L^{-1} was prepared, diluted to 12 solutions of 50 to 600 mg L^{-1} in volumes of 10 mL. Absorption quantifications were made at a wavelength of 280 nm. All calibration curves were obtained from Origin, as well as its equations and its coefficients of determination (R^2). Limits of detection (LD) and quantification (LQ) calculations for all calibration curves were performed based on the International Union of Pure and Applied Chemistry [33].

Estimation of Condensed Tannins in *Eucalyptus citriodora* Bark Fibers

Based on the properties of tannins to absorb radiation in the UV–Vis spectrum between 250 and 300 nm, with peaks at approximately 265 nm related to hydrolyzable tannins and 280 nm to condensed ones [34], GA and TA were used as comparison agents given their chemical and spectral characteristics in order to base the estimation of the tannic content on the extract of natural fibers. The way of determining condensed tannins was the comparison of the UV–Vis spectrum of the natural fiber extract to that of TA. Despite being predominantly a mixture of polygaloyl-glucose and, therefore, hydrolysable tannin, TA has a maximum absorption wavelength characteristic of chromophores in condensed tannins, being a good reference candidate for their identification, as well as the absorbance of the extract at 280 nm was applied to the equation of the TA calibration curve. To determine the hydrolyzable tannins, the spectrum of the extract was compared to that of GA and its absorbance at 265 nm applied to the equation of the calibration curve for GA. All measurements were performed in triplicate and the vegetable condensed tannin of *Acacia mearnsii* (Mimosa) was also analyzed as a purely qualitative pattern.

Chemical Treatments of *Eucalyptus citriodora* Bark Fibers

Hydrolysis Treatments

Three variants of the hydrolysis treatment of eucalyptus bark fibers were applied. First, 2.0 g were washed

according to the aqueous extraction process already described; two other portions of 2.0 g each underwent acid and alkaline electrolytic treatment according to Santos [35]. Thus, one received 25 mL of 0.1 mol L^{-1} NaOH solution (MERCK, 97.0% purity) for basic hydrolysis and another 25 mL of 10% v/v HNO3 solution (MERCK, 65.0% purity) for acid hydrolysis. Both mixtures were in contact for 2 h at 20 ± 1 °C, then they were filtered and washed in a Soxhlet extractor at a temperature of 90 °C until obtaining residual water without color and with pH 7. The product obtained was again dried in an oven (at 103 ± 2 °C).

Immobilization of Tannins

Obtaining fibers with their own immobilized component tannins is a fourth variant to study the removal capacity of treated fibers. The method was adapted from Luzardo [26] from the following steps: 2.0 g of the fibers were poured into a 250 mL beaker containing a 3.0 mL formaldehyde (CH_2O) solution 37% volume (Synth), 8.0 mL deionized water and 0.2 mL hydrochloric acid (HCl) PA 37% (Neon). The mixture was kept under gentle manual agitation, using a glass rod, for 20–30 min, at room temperature (20 ± 1 °C) and then gradually heated in an oven to 103 ± 2 °C until the excess aqueous was evaporated. After this time, the solid material was washed in the Soxhlet extractor at a temperature of 90 °C for 2h30 min. The product obtained was again oven dried (at 103 ± 2 °C) and ground in a pistil to particles of approximately 45 mesh.

Synthesis of Tannin Resin and Treated Eucalyptus Bark Fibers

Brazil is already commercially exploring the potential of species for the extraction of commercial tannins, such as Acacia mearnsii, from which mimosa tannin is extracted by TANAC S.A. and which was applied to the preparation of adsorbent variants 5–9. The enrichment of eucalyptus fibers with mimosa tannin sought to make BSA-adsorbent bonds more efficient by reducing steric impediments. The resin synthesis was carried out following the same methodology mentioned above for the immobilization of tannins in the fibers, adapting it according to Luzardo and collaborators [28], thus, tannin mimosa was added to the fibers of the eucalyptus bark for a polycondensation reaction in a solution of formaldehyde, water and hydrochloric acid. Five resin variants were prepared. The studied percentages between tannin and eucalyptus were, respectively, (50–50; 10–90 and 100–0), among the 10–90 proportions, three different fiber particle sizes were tested, 20, 48–65 and 100–150 mesh.

Physical and Chemical Characterizations of the Resin

All physical characterization experiments of the resin were carried out in triplicate weighing 0.5 g on an analytical balance. The moisture content was obtained by gravimetric analysis via drying of the samples, the degree of swelling was measured from the amount of water absorbed per gram of dry sample, the apparent density analyzes considered the total volume of the sample, including empty space, intragranular pores, whereas the determination of the packing density considers only the volume of the set of grains that make up the sample packed by an aliquot of water and the specific mass was determined by adding a portion of the weighed dry resin to 5 mL of deionized water and measuring the volume of water displaced, all these properties were calculated according to Marhol [36]. The chemical characterizations of resin, tannin mimosa and fibers from the bark of *Eucalyptus citriodora* were performed by obtaining UV–Vis spectra between 220 and 320 nm of its aqueous extracts, using deionized water as a blank for each sample, enabling the identification of maximum and minimum absorption related to its tannic components and to characterize the prepared resin, BSA and post-adsorption resin solid and dry aliquots of the samples were studied by spectra between 650 and 4000 cm^{-1} by Fourier Transform Infrared Attenuated Total Reflectance Spectroscopy (FTIR-ATR) in PerkinElmer Spectrum 400 FT-IR/FT-NIR Spectrometer equipment. The spectra obtained are averages of 10 scans, obtained with a resolution of 4 cm^{-1} and were processed using Spectrum software from PerkinElmer. This enabled the recognition of the active functional groups of the analytes.

BSA Protein Adsorption Studies

BSA adsorption capacity studies were applied to each of the nine prepared adsorbents, thus, they were used to rank the best among them. The studies were carried out in triplicate and under the monitoring of the analytical blank, which consisted of a fourth beaker with all components in the same proportions, excluding, however, the BSA. Its treatment was the same as that given for the units that contained the analyte and its absorbance was measured and subtracted from the total absorption of those replicates that contained the protein. The mass of each adsorbent tested was 0.05 g, stored solid state in a 250 mL beaker, accommodated on the Ethik Technology digital orbital shaking table programmed to stir at 70 rpm (0.1372 g) for 30 min, a time that was later studied by the kinetics of adsorption. Thus, 10 mL of BSA solution with known concentration was poured onto the adsorbent, as well as deionized water on the blank. At the end of the process, the solids were separated by a qualitative filter (Unifil) and the solution centrifuged in Centrifuge SL-700 SOLAB for 5 min at 3000 rpm (1844 g). The supernatant

then had absorption measured in UV–Vis at 280 nm, which applied the equation of the BSA calibration curve, determined the protein concentration at the end of the adsorption process. All experiments were carried out at a temperature of 20 ± 1 °C. The equilibrium adsorption capacity value (q_e) was calculated for each replica by Eq. 1, giving an average result for the different studied variables, in the same way, Eq. 2 was applied to calculate the percentage of removal q% [37].

$$q_e = \frac{(C_0 - C_e)V}{m} \tag{1}$$

where q_e is the equilibrium adsorption capacity (mg g^{-1}), C_0 initial adsorbate concentration (mg L^{-1}), C_e equilibrium adsorbate concentration (mg L^{-1}), V volume of adsorbate solution (L) in the mass of the adsorbent (g).

$$q\% = \frac{C_0 - C_e}{C_0} 100 \tag{2}$$

Influence of pH Variation on Adsorption

The study methodology for the influence of pH variation on adsorption follows as above, varying only the solvent of the BSA solution, where aqueous solutions of different buffers prepared according to the Henderson-Hasselbalch equation: PBC buffer (Phosphate-Borate-Citrate) 5×10^{-3} (KH_2PO_4 PA Synth, H_3BO_3 PA VETEC and $C_6H_8O_7$ PA Synth) was used to obtain different pH's (4.0, 5.0, 6.0, 7.0, 8.0 and 9.0) adjusted using NaOH 1×10^{-1} mol L^{-1} (MERCK, 97.0% purity) or 1×10^{-1} mol L^{-1} HCl (37% Neon) and measured by a BEL digital pH meter. Tests were also performed with acetate buffers 1×10^{-2} mol L^{-1} for pH's 3, 4 and 5 (CH_3COOH Glacial USP 100% and CH_3COONa PA Synth) and phosphate 1×10^{-2} mol L^{-1} for 6, 7 and 8 (Na_2HPO_4 PA and $NaH_2PO_4 \cdot H_2O$ PA Synth).

Study of Adsorption Kinetics

The experiments were carried out with different contact times (3, 7, 10, 20, 30, 40, 75 and 90 min) between the adsorbent and the BSA solution, prepared according to the results of the study of the influence of pH variation on adsorption. The relationship between contact time and adsorption capacity was studied using nonlinear theoretical models of pseudo order and linearized Elovich equation. These studies were complemented from the intraparticle diffusion analyzes via linear equation, with their mathematical expressions (Eqs. 3, 4, 5 and 6) in accordance with Largitte and Pasquier [38].

$$\text{Pseudo} - \text{firstorder} : q_t = q_e(1 - \exp(-k_1 t)) \tag{3}$$

$$\text{Pseudo} - \text{secondorder} : q_t = \frac{q_e^2 k_2 t}{1 + q_e k_2 t} \tag{4}$$

$$\text{Elovichequation} : q_t = \frac{1}{\beta}\ln(\alpha\beta) + \frac{1}{\beta}\ln(t) \tag{5}$$

$$\text{Intraparticlediffusion} : q_t = k_d t^{\frac{1}{2}} + I \tag{6}$$

where q_t is the adsorption capacity at time t (mg g^{-1}), k_1 is a pseudo first order adsorption rate constant (min^{-1}), t is the contact time of the adsorbent with the contaminated solution (min), k_2 pseudo second order adsorption rate constant (g mg^{-1} min^{-1}), α initial adsorption rate constant (mmol g^{-1} min^{-1}), β parameter related to the extent of surface coverage and energy of activation for chemisorption (g $mmol^{-}1$), k_d is the intraparticle diffusion rate constant (mg g^{-1} $min^{1/2}$) and I the variable related to boundary-layer effects such as thickness.

Study of the Adsorption Isotherm

The study was carried out with a fixed mass of the ideal adsorbent (0.05 g), varying 8 initial concentrations of BSA adsorbate from 100 to 430 mg L^{-1}, keeping the temperature controlled at 20 ± 1° C and applying the ideal time to reach the balance according to the kinetic study. The experimental isotherms were applied in theoretical models to determine the maximum adsorption capacity and the best theory to simulate the experimental data. In order to analyze the data by more limited models regarding the type of adsorbent surface, Langmuir [39] (Eq. 7) and Freundlich (Eq. 8) were applied according to non-linear mathematical expressions Foo and Hameed [40].

$$q_e = \frac{q_m K_L M_e}{1 + K_L M_e} \tag{7}$$

$$q_e = K_F M_e^{\frac{1}{n}} \tag{8}$$

where q_m represents the maximum adsorption capacity (mg g^{-1}), K_L constant of the Langmuir isotherm (L mg^{-1}), M_e equilibrium concentration of chemical species (mg L^{-1}), K_F constant of the Freundlich isotherm ((mg g^{-1})/(L mg^{-1})1/n) and n is the heterogeneity factor of the Freundlich isotherm.

Completing the study, the data were analyzed by hybrid models of the first ones, Redlich–Peterson (Eq. 9) and Sips (Eq. 10), applying nonlinear mathematical expressions following consolidated models reported by Neris [25].

$$q_e = \frac{K_R M_e}{1 + a_R M_e^g} \tag{9}$$

$$q_e = \frac{q_s a_S M_e^{\frac{1}{n_S}}}{1 + a_S M_e^{\frac{1}{n_S}}} \tag{10}$$

where K_R constant of the Redlich-Peterson isotherm (L g^{-1}), a_R constant of the Redlich-Peterson isotherm (mg $L^{-1})^g$, g exponent of the Redlich-Peterson isotherm (ideal value $0 \leq g \leq 1$) n_s Sips isotherm exponent, a_S constant of the Sips isotherm related to the adsorption energy (L g^{-1}) and q_s is the adsorption capacity obtained by the Sips isotherm (mg g^{-1}).

Treatment of Experimental Data

All data generated were treated statistically, the computer program Origin was used. Calibration curves were determined under conditions of determination coefficient (R^2) closest to unity, in addition, isothermal and kinetic parameters were determined for chi-square values (χ^2) lowest for each data set. Statgraphics was also used to generate all the statistical data, such as the Ducan tests to establish average comparison results.

Results and Discussion

Vegetable tannins are soluble in water and the aqueous extracts of *Eucalyptus citriodora* bark fibers, those that had their tannins immobilized and resin composed of 10% fibers and 90% mimosa tannins were analyzed by UV–Vis spectroscopy and compared with reference compounds (Fig. 1). The main group of chromophores in these extracts is the aromatic rings, which in condensed tannins present two absorption peaks, one in a region close to 200 nm and another close to 280 nm, while the hydrolysable ones absorb in peaks of approximately 210 nm and 270 nm [34].

In all spectra peaks characteristic of the presence of tannins between 250 and 300 nm were identified. Among the reference solutions, gallic acid (GA) peaked at 265 nm, tannic acid (TA) and tannin mimosa at 280 nm. In natural fibers, the most evident peak was at 275 nm with the 265 nm region superimposed, indicating the presence of condensed and hydrolysable tannins. On the other hand, in the spectrum of the resin extract composed of 10% fiber 90% tannin mimosa and in the fibers that underwent the immobilization process of their own tannins, there was a loss of characteristic absorption bands, however, in the region of 265 nm, related to hydrolyzable tannins, the absorbance was more expressive than in the 280 nm range, indicating that

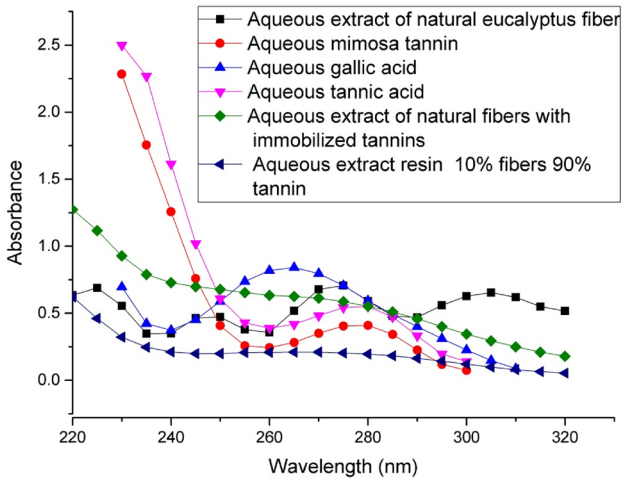

Fig. 1 UV–Vis spectra of reference tannic compounds, extracts of natural eucalyptus fibers and those modified by polycondensation

the synthesized products reached greater insolubility of the immobilized condensed tannins.

Based on the equations of the calibration curves prepared for TA (A = 0.0099C + 0.0091) and GA (A = 0.0433C—0.0163) (Table 1), the masses of condensed tannins were measured (CT) and hydrolysables (HT) extracted in relation to the dry natural fiber mass of the bark of *Eucalyptus citriodora*, the same relation was used to quantify the total soluble solids (TSS). The mean percentages ± standard deviation calculated were $0.0905 \pm 2 \times 10^{-4}$ for CT, $0.0190 \pm 4.1 \times 10^{-5}$ for HT and $11{,}789 \pm 2 \times 10^{-1}$ TSS. The estimates are representative of the studied sample, as plant species suffer compositional variations due to climatic interference, maturation, location of the sample collected on the tree, among others. The determination of TSS content illustrates the importance of aqueous extraction of lignocellulosic fibers, which adds value to them for commercial and analytical applications, as it reduces the possibility of interfering both in the solution treatment and in the final quantification of the analyte.

The studies indicated that the tannin–formaldehyde reaction is possible and that eucalyptus fibers carry a tannin content that also enriched the resin. The tannin immobilization tests, as well as the resin production were based on the polycondensation reaction of polyflavonoid tannins with formaldehyde in an acidic medium, which occur preferentially in the C6 and C8 positions in the A ring, generating formaldehyde itself as common by-products of the reagents and water [41]. It can be said that the reaction helps itself by shifting the balance towards the formation of more products. This makes it faster and more profitable; however, it generates resins with a high degree of hardness, which requires mills to generate smaller grains, as did Luzardo [28]. To prepare a less rigid resin, good results were found by adding in the reaction of lignocellulosic fibers an amount of water

sufficient to humidify the solid reactants, so that the aqueous medium slowed the reaction making the product susceptible to be macerated with a pistil.

Resin variants, in addition to different fiber treatments, had the mean percentage of BSA removal in solution measured based on initial and equilibrium concentrations (Fig. 2), quantified by measuring the absorbance at 280 nm applied to the equation for the calibration curve. BSA in UV–Vis ($A = 6.24 \times 10^{-4}C - 4.04 \times 10^{-4}$) (Table 1). The adsorbent variants prepared and tested were nine and Table 2 details the composition of each one of them.

The best analytical responses for treated fibers were for immobilized tannins, followed by resins composed of 10% for fibers and 90% for tannins, in this case, the ideal result for further research was obtained using the smallest fiber particle size (between 100 and 150 mesh), probably the positive influence is the greater contact surface and the uniformity between the particles of tannin extract and ground fiber from the eucalyptus bark. The ideal ratio of reagents to resin was 0.9 g of tannin mimosa; 0.1 g of eucalyptus fibers; 1.5 mL of 37% formaldehyde; 0.1 mL of 37% hydrochloric acid and 2.5 mL of deionized water. 71.6 ± 2.78% removal

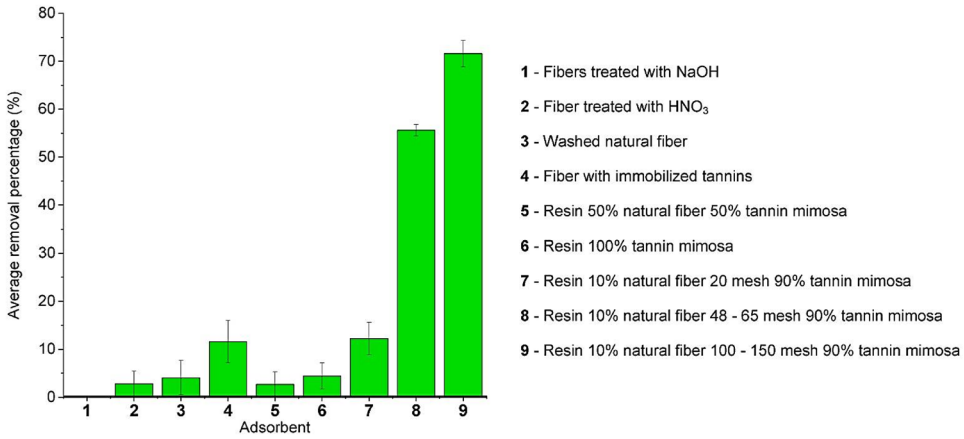

Fig. 2 Average percentages of BSA removal per adsorbent solid prepared according to Table 2

Table 1 Summary of adsorbent variants and their compositions

Adsorbent variant	Preparation components	Washed product, pH 7, dry and grounded
1	2.0 g of eucalyptus fibers ground to 20 mesh + 25 mL of NaOH 0.1 mol L^{-1} at rest for 2 h at 20 ± 1 °C	Fibers with alkaline electrolytic treatment
2	2.0 g of eucalyptus fibers ground to 20 mesh + 25 mL of 10% v/v HNO_3 at rest for 2 h at 20 ± 1 °C	Fiber with acid electrolytic treatment
3	2.0 g of eucalyptus fibers ground to 20 mesh subjected to aqueous extraction in the Soxhlet extractor	Washed fiber
4	2.0 g of eucalyptus fibers ground to 20 mesh + 3.0 mL of 37% formaldehyde + 8.0 mL of deionized water and 0.2 mL of 37% HCl. Light agitation between 20 and 30 min	Fiber with its natural immobilized tannins
5	1.0 g of eucalyptus fibers ground to 20 mesh + 1.0 g of mimosa tannin + 3.0 mL of 37% formaldehyde + 8.0 mL of deionized water + 0.2 mL of 37% HCl. Light agitation between 20 and 30 min	Resin 50% fiber 50% mimosa tannin
6	2.0 g mimosa tannin + 3.0 mL 37% formaldehyde + 8.0 mL deionized water + 0.2 mL 37% HCl. Light agitation between 20–30 min	Resin 100% mimosa tannin
7	0.2 g of eucalyptus fibers ground to 20 mesh + 1.8 g of mimosa tannin + 3.0 mL of 37% formaldehyde + 8.0 mL of deionized water + 0.2 mL of 37% HCl. Light agitation between 20 and 30 min	Resin 10% fiber 20 mesh 90% mimosa tannin
8	0.2 g of eucalyptus fibers ground between 48 and 65 mesh + 1.8 g of mimosa tannin + 3.0 mL of 37% formaldehyde + 8.0 mL of deionized water + 0.2 mL of 37% HCl. Light agitation between 20 and 30 min	Resin 10% fiber 48–65 mesh 90% mimosa tannin
9	0.2 g of eucalyptus fibers ground between 100 and 150 mesh + 1.8 g of mimosa tannin + 3.0 mL of 37% formaldehyde + 8.0 mL of deionized water + 0.2 mL of 37% HCl. Light agitation between 20 and 30 min	Resin 10% fiber 100–150 mesh 90% mimosa tannin

Table 2 UV–Vis calibration curves data for BSA, gallic acid and tannic acid

	BSA	Gallic acid	Tannic acid
Absorption band	280 nm	265 nm	280 nm
Intercept	$-4.04\times10^{-4}\pm2.75\times10^{-3}$	$-1.63\times10^{-2}\pm5.2\times10^{-3}$	$9.1\times10^{-3}\pm3.6\times10^{-3}$
Slope	$6.24\times10^{-4}\pm7.47\times10^{-6}$	$4.33\times10^{-2}\pm4.18\times10^{-4}$	$9.9\times10^{-3}\pm5.86\times10^{-5}$
R-Square(COD)	0.9986	0.9993	0.9997
LD	2.48	0.05	0.16
LQ	8.27	0.17	0.52

percentage was achieved in a concentrated solution of BSA 260 mg L^{-1}. This is an encouraging result. The literature points to traditional techniques for removing proteins from waste solutions, such as ultrafiltration ranging from 30 to 95% or precipitation between 50 and 81% of yield [7].

The characteristics and treatments of the resin components with the best experimental response for the adsorption of BSA (10% fibers 100–150 mesh 90% tannin mimosa) conferred particular physical properties. Swelling degree, bulk density and pack density with mean values ± standard deviations of 0.0624 ± 0.0087 g g^{-1}, 0.3872 ± 0.0029 g cm^{-3} and 0.2517 ± 0.0019 g cm^{-3}, respectively, and specific mass of 1.6779 ± 0.0126 g cm^{-3}, which is noteworthy for being greater than 1 g cm^{-3} (reference of pure water), together with the low values of the other properties, indicate low water absorption, high packaging capacity and to remain under the water flow in treatment, avoiding greater losses of the adsorbent in the process. These data are advantageous for adsorption and future applications in columns, as they facilitate water flow, thus reducing flow loss [28].

The synthesized resin bears the characteristics of its components, however, bands are displaced disappear or appear. The component with the highest concentration in the resin is mimosa tannin, mainly composed of condensed tannins, followed by eucalyptus fibers, mostly composed of lignin, cellulose, hemicellulose and tannins. The spectra are in agreement with those already reported in the literature. As well as in the tannin mimosa resin-coconut fibers-carbon nanotubes [28], in this tannin mimosa-eucalyptus fiber resin, a new band appeared between 600 and 700 cm^{-1}, here at 672 cm^{-1}, corresponding to the out-of-plane deformation of hydroxyl groups (OH) in hydrogen bonds. The band at 780 cm^{-1} is characteristic of mono and disubstituted benzenes, corresponding to out-of-plane deformation in the case of aromatic compounds, it can also be related to the displacement of bands between 815 and 819 cm^{-1} related to para-substituted benzene with out-of-plane CH deformations appearing in mimosa tannin and corresponding to proanthocyanidins (flavonoids with two or three hydroxyl groups in the B ring) and may be present in eucalyptus bark complex oligomeric condensed tannin compounds [21].

Both mimosa tannin and eucalyptus have a band between 1029 and 1032 cm^{-1} suggesting the presence of deformation in the CO bonds of the heterocyclic ring present in condensed tannins [21]. In the resin spectrum, this band remains expressive, shifted to 1082 cm^{-1}. These two components showed peaks in the resin spectrum in characteristic bands, close to 1200, 1300, 1400 and 1600 cm^{-1}, which suggest, respectively, the presence of phenolic groups in eucalyptus; stretching the phenolic hydrogen of tannic compounds; angular deformation of C=O and OH bonds of carboxylic acid in eucalyptus; and CC conjugate bond vibrations in phenolic aromatic ring or out-of-plane OH vibration. These same characteristics were pointed out by Sartori [20], Correia [42] and Santos [35] in different species of eucalyptus and in their comparisons with reference tannins.

The spectrum of the adsorbed BSA resin has a higher percentage of transmittance, which indicates less freedom of vibration of the functional groups previously characterized in the resin and BSA spectra, demonstrating the occurrence of a strong interaction between them, possibly by complexation, as suggested by Haslam [17]. The lack of bands in the region between 800 and 655 cm^{-1} in the spectrum of the adsorbed BSA resin is noteworthy. In the spectrum of pure resin, this area indicates the existence of OH and CH groups characteristic of tannins, whereas for BSA, according to Kong and Yu [43], the bands between 537 and 606 cm^{-1} indicate angular deformation outside the plane of C=O, 625−767 cm^{-1} are of angular deformation of OCN and 640−800 cm^{-1} angular deformation out of the plane of NH, added to these other functional groups have lost characteristics, such as the stretches of NH in 3100 cm^{-1} and of the C=O at 1600−1690 cm^{-1}.

The high transmittance exhibited by the spectrum of the resin adsorbed by BSA can lead to an estimate of the low concentration of previously identified functional groups, which leads to a practical interpretation of the computational investigation by Hernándes et al. [31] which concluded that tannin-amino acid interactions, regardless of the amino acid group, are hydrophobic and hydrophilic simultaneously, occur between hydroxyl groups, ether and protons of the rings of flavonoid monomers and amine and/or amide groups, carboxylic acid and chains CH of amino acids. In this work, although peaks in bands between 1080 and 1607 cm^{-1} common to pure resin were identified in the post adsorption resin, as well as the band at 3750 cm^{-1} of

BSA, the other bands disappeared and many are undefined between 1467 and 1607 cm^{-1} and 1607–2500 cm^{-1}, which probably refer to amino acid traces, all these bands showed low intensities. This characterizes strong resin-BSA interactions, including hydrogen bonds between the amide and/or amine and carboxylic acid groups of the amino acids and the phenolic OH groups of the resin plus other possible interactions through the CH and CO groups of the resin and CH of the protein peptide chains.

In recent experimental work, collagen hydrolysates were reacted with a commercial solution of mimosa bark tannin extract. According to Pizzi [23] covalent bonds predominated and appeared to occur between the two materials by reactions between the phenolic groups –OHs of tannin and the amino groups of the non-skeletal side chains of arginine and also by reactions of the –COOH groups of glutamic and aspartic acids on the aliphatic alcohol-OH in the C3 site of tannin heterocycle flavonoid units. The five constituents in the highest percentages in BSA are leucine, glutamic acid, lysine, alanine and aspartic acid [30]. In the studies by Hernández et al. [31], lysine, aspartic acid, glutamic acid, histidine and arginine were the amino acids that interacted with more strength and stability with both resorcinolic and phloroglucinolic tannins. Looking at just this category of amino acids there is a 60% similarity between the five most abundant amino acids in BSA and the five best condensed tannin complexes. In terms of chemical characteristics, none of these mentioned amino acids has an aromatic group and only histidine has a closed chain in its structure. Probably the smallest effect of the steric hindrance that would limit the amino acid-tannin interaction is related to this ranking of the best amino acids.

In terms of the groups of amino acids that make up proteins, Hernández and collaborators [31] stated that the best results are obtained for acidic hydrophilic and basic hydrophilic, which are in relevant percentages in BSA, together are 33.98% of each macromolecule. The aliphatic amino acids are the most abundant in BSA, 34.63%, and leucine is the most abundant amino acid in the biomolecule. Hernández et al. [31] showed that complexes with leucine are the most stable of their group for both flavonoid species.

The functional groups that are components of the resin and also of the protein are electrostatically altered as a function of pH changes. The formation of the tannin-protein complex is pH dependent and it is maximum and ideal around the isoelectric point (pI) of the protein [6] which for BSA is in the pH range of 4.9–5.5 [14]. Here tests were carried out in the pH range 3–9. Only at pH 4, 5 and 6 the results were favorable, but not able to improve the result achieved in the buffer-free medium. According to Latour [15], cations and anions of salts dissociated in solution diffuse at a much faster rate than a protein, thus, before the protein-adsorbent interaction, the charged functional groups, both on the protein and on the surface of the adsorbent material, are complexed and occupied with counterions. It is noteworthy that at pH 5 both, regardless of the buffer used, the removal percentage was favorable, a condition related to the pI of the protein. Based on these results, the BSA solutions continued to be prepared solely with deionized water, which gave it a pH of $\sim 5.32 \pm 0.02$.

The kinetic and successively isothermal studies were carried for the adsorption of the resin that showed the highest percentage of BSA removal, consisting of 90% mimosa tannin and 10% eucalyptus bark fibers in smaller granulometry between 100 and 150 mesh, out with experiments in a controlled temperature environment at 20 ± 1 °C, under constant agitation of 70 rpm and in an aqueous medium free of ions. The kinetic data was applied to the multiple comparison procedure to determine which means had Fisher's least significant difference (LSD) with a confidence level of 95.0%, concluding that there were no statistically significant differences for the experimental means of q from 7 min onwards, Fig. 4a. This short time to reach the adsorption equilibrium is an advantage for the practical application of the resin.

The Chi-square statistical test (χ^2) of the parameters of the kinetic models shown in Table 3 was conclusive for indicating smaller discrepancies between the experimental values and those theoretically predicted for the pseudo first order model. Anirudhan et al. [44] synthesized an adsorbent composed of tannin for BSA and the system was better represented based on the solid surface capacity, therefore, in the pseudo-first order model. Here, the experiments show that the BSA-resin adsorption increased with the increase in the concentration of tannins and greater contact surface in the adsorbent, on the other hand, it decreased with the increase of the ionic charge in the medium, it is concluded that the composition and availability of the surface active sites are crucial in this adsorption, as shown by the post adsorption resin spectrum in Fig. 3b.

The pseudo first order model is insufficient to address all the specificities of protein adsorption, so the analysis via intraparticle diffusion is complementary. Figure 4b illustrates three stages of adsorption: the first minute, where, possibly, the highest concentration of proteins in the medium causes them to migrate to the solid surface at a high rate from the first seconds of physical contact under agitation, winning and taking the place of the water that surrounded and interacted with the solid. The second stage of intraparticle diffusion was the 6 min where the protein diffused to pores and cracks found in the structure of heterogeneous particles and without uniformity of the adsorbent, these data correlated well with the model, with $R^2 = 0.9994$ and low χ^2 (Table 3), which did not occur for the last stage after 7 min, this consists of the slow phase, probably controlled by adsorption/desorption equilibrium forces, where the adsorbent reaches its maximum adsorption capacity.

Table 3 Kinetic and isothermal parameters against theoretical models

Kinetic parameters				Isotherm parameters (20 °C)			
Pseudo-first order				Langmuir			
q	26.9 ± 0.08	R^2	0.9999	q_m	26. 7 ± 0.29	R^2	0.9810
k_1	1.18 ± 0.09	χ^2_{red}	0.3076	K_L	0.08 ± 0.01	χ^2_{red}	1.0523
Pseudo-second order				Freundlich			
q	27. 5 ± 0.20	R^2	0.9998	K_F	10.2 ± 0.90	R^2	0.9550
k_2	0.10 ± 0.02	χ^2_{red}	0.9753	N	5.96 ± 0.61	χ^2_{red}	2.4933
Elovich equation				Redlich-peterson			
A	$2.9\times10^{16}\pm7.0\times10^{17}$	R^2	0.9990	K_R	2.73 ± 0.72	R^2	0.9858
B	1.54 ± 0.93	χ^2_{red}	3.9682	a_R	0.13 ± 0.06	χ^2_{red}	0.9406
				G	0.95 ± 0.04		
	Intraparticle diffusion			Sips			
K_{d1}	13.2 ± 0.32	K_{d2}	0.23 ± 0.23	q_s	28.6 ± 1.98	R^2	0.9873
R^2_1	0.9994	R^2_2	0.1964	a_S	0.15 ± 0.06	χ^2_{red}	0.8461
$\chi^2_{red\ 1}$	0.0221	$\chi^2_{red\ 2}$	0.2529	n_S	1.39 ± 0.34		
				$q_{experimental}$		25.3 ± 0.68	

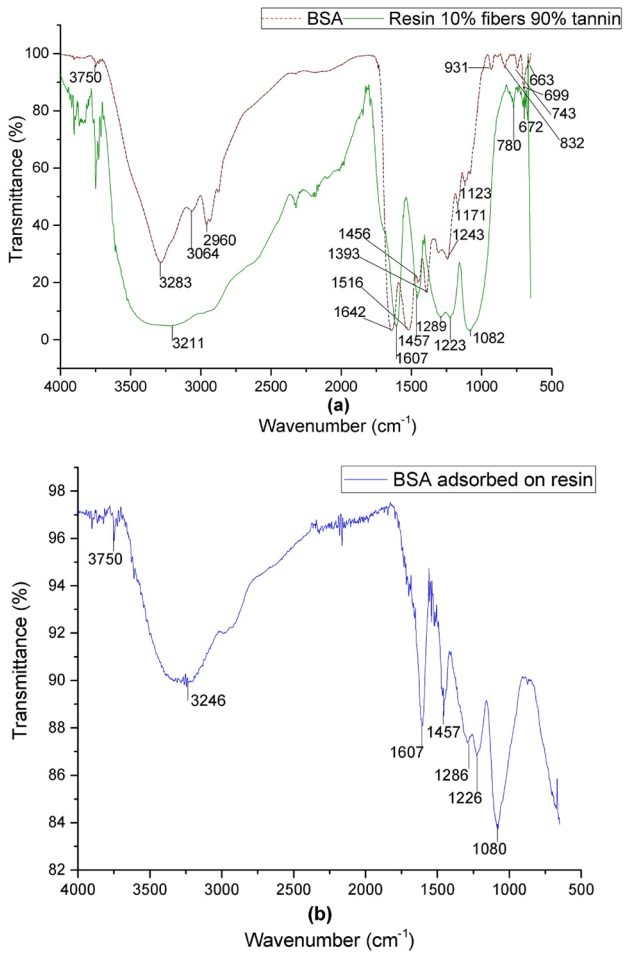

Fig. 3 FTIR-ATR spectra of BSA and resin before (**a**) and after adsorption (**b**)

According to Bazzaz et al. [16], mathematically, if the graphs of q_t versus $t^{1/2}$ pass through the origin, then intraparticle diffusion is the only step to control the adsorption rate. However, none of the straight lines (Figure 4b) passed through the origin, so other factors can control the adsorption of BSA by the resin, such as the occupation of the adsorbent surface by the unfolding of adsorbed proteins [15], thus, spaces and consequently, the active sites are quickly filled with the same amount of proteins.

The adjustments of the data to the adsorption isotherm models (Fig. 4c) and (Table 3) prove that the experimental phenomenon occurs through adsorption. Given the heterogeneous nature of the resin, the models that best converged with the data were those based on the combination of the Langmuir and Freundlich models, therefore, the Redlich Peterson and Sips models, with the latter offering the best adjustments for the experimental data with higher R^2 and lower χ^2 values, based on the theory that the active sites of the adsorbent have heterogeneous energies. However, the Langmuir model better determines the maximum adsorption capacity q_{mL}, 26.7 ± 0.29, with a smaller calculated standard deviation and a value closer to that obtained experimentally in the equilibrium adsorption range.

Table 4 compares the results of this work with others already published for the BSA. Some commercial or developing materials have q_{mL} greater than that achieved here, others are similar or smaller. The comparison of the resin functionalized with tannic acid by Li et al. [45] with the one described in this work, the second has adsorption capacity for the larger BSA. It is added that all works, except this one, needed a buffer to find the best adsorption pH and none of them had adsorption equilibrium time as low as the resin described here. The fast kinetics of the resin

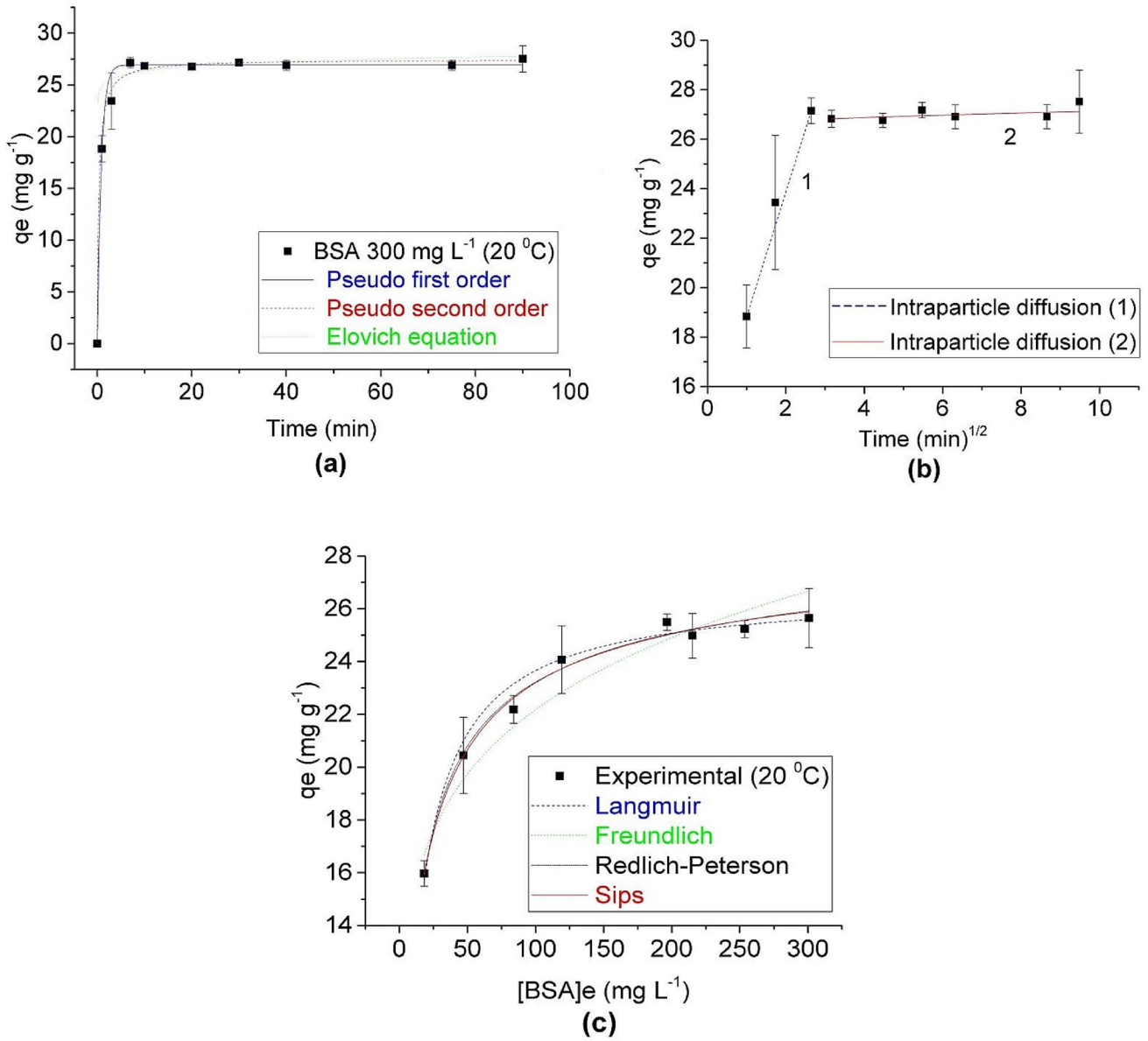

Fig. 4 Theoretical and experimental models of adsorption kinetics (**a**) and (**b**) and adsorption isotherms (**c**)

tannin-eucalyptus fibers is a differential that adds greater efficiency in adsorption.

Conclusion

The results obtained here showed that it is possible to immobilize tannins inside natural lignocellulosic fibers, as well as synthesize tannin–formaldehyde polymeric resin with percentage of natural fiber. The resin showed good removal of BSA molecules from water with good adsorption capacity in short contact time. The best removal percentage by pH was obtained in the BSA pI range, ~ 5.32 ± 0.02, using BSA solution in deionized water.

The synthesized resin can reach a maximum adsorption capacity within 7 min. The best fit for the isotherm corresponds to the Sips model, however, the Langmuir model was more suitable for determining the maximum adsorption capacity of BSA, ~ 26.7 mg g^{-1}.

The hypothesis that the functional groups of the BSA amino acids could strongly interact with the active sites of the resin tannin-eucalyptus fibers via hydrogen bonds, hydrophobic and hydrophilic interactions proves positive, as the transfer of protein mass in solution to the surface and porosities of the adsorbent was the mechanism for

Table 4 Comparison of Langmuir adsorption capacities for BSA of different commercial and developing adsorbents

Adsorbent	pH/time/ °C	q_{mL} (mg/g)	References
Commercial resin Nuvia cPrime Nuvia with p-aminohippuric acid	pH 4.0/4 h/ 25 °C	122.6	[46]
Allyl agarose-bromide-N-bromosuccinimide-tryptamine resin	pH 5.0/20 min/25 °C	59.74	[47]
	pH 6.0/20 min/25 °C	51.81	
	pH 7.0/20 min/25 °C	46.80	
Electrophied cellulose nanofiber felt	pH 8.0/24 h/–	40	[48]
Commercial regenerated cellulose membrane	pH 8.0/24 h/–	33.5	[48]
Commercial resin Nuvia cPrime Nuvia with p-aminohippuric acid	pH 6.0/4 h/25 °C	28.1	[46]
Resin taninn-eucalyptus fibers	pH 5.3/7 min/ 20 °C	26.7	This work
Regenerated cellulose microfiber felt	pH 8.0/24 h/–	14.5	[48]
Cotton ball	pH 8.0/24 h/–	15.5	[48]
Chitosan-tannic acid resin	pH 6.0/22 min/25 °C	1.094	[45]
	pH 6.0/22 min/35 °C	1.487	
	pH 6.0/ 22 min/45 °C	1.694	

determining the adsorption process instead of chemisorption, as the data converged well with the pseudo first order and intraparticle diffusion models.

The experiments show that the BSA-resin adsorption increased with the increase in the concentration of tannins and greater contact surface in the adsorbent and decreased with the increase in the ionic charge in the medium, it is concluded that the composition and availability of active sites on the surfaces are crucial in this adsorption.

Based on the results obtained about its adsorption capacity, it is possible to conclude that the new synthesized resin is a good alternative for future use in the treatment of fluids containing proteins or protein species, which contain higher percentages of amino functional groups in their structure. The expectation is that hospital, laboratory, dairy, slaughterhouse, domestic fluids, among others, are promising candidates for possible protein decontamination. Given the polymeric nature of the resin, it is promising for testing incorporation into other materials, including polymeric ones, in the generation of active products for the adsorption of protein structures.

The combination of two natural products, produced and/or distributed worldwide, such as tannins and fibers from eucalyptus bark obtained as by-products of wood production, make the product developed, in addition to being innovative, with sustainable potential, easy replication and with low cost, both for synthesis and application.

Acknowledgements The authors are grateful to State University of Santa Cruz (UESC) and the Foundation for Research Support of the State of Bahia (FAPESB). L.C.S. and F.G.V. are National Council for Scientific and Technological Development (CNPq) research fellows.

Author Contributions DSD: Methodology, Validation, Writing—Original Draft. FHML: Methodology, Conceptualization, Writing—review & editing. FGV: Conceptualization, Resources, Project administration. ONA: Methodology, Data Curation, Software. GDRZB: Methodology and validation. GGN: Methodology and validation. TBVA: Methodology and validation. LCS: Conceptualization, Writing—review & editing and Supervision.

Funding The authors have not disclosed any funding.

Declarations

Competing interest The authors declare no competing interests.

References

1. Jin M, Shi J, Zhu W, Yao H, Wang D (2020) Polyssacharide based biomaterials in tissue engineering: a review. Tissue Eng Part B 27:604–626. https://doi.org/10.1089/ten.teb.2020.0208
2. Zhao Y, Shi L, Kuang H, Xu C (2020) DNA-driven nanoparticle assemblies for biosesning and bioimages. Top Curr Chem 378:267–299. https://doi.org/10.1007/s41061-020-0282-z
3. Salay LC, Carmona-Ribeiro AM (1999) Wetting of SiO_2 surfaces by phospholipid dispersions. J Adhes Sci Technol 13:1165–1179. https://doi.org/10.1163/156856199X00857
4. Salay LC, Carmona-Ribeiro AM (1998) Synthetic bilayer wetting on SiO_2 surfaces. J Phys Chem B 102:4011–4015. https://doi.org/10.1021/jp973295k
5. Salay LC, Petri DFS, Nakaie CR, Schreier S (2015) Adsorption of the antimicrobial peptide tritrpticin onto solid and liquid surfaces: Ion-specific effects. Biophys Chem 207:128–134. https://doi.org/10.1016/j.bpc.2015.10.004
6. Coglitore D, Janot JM, Balme S (2019) Protein at liquid solid interfaces: toward a new paradigm to change the approach to design hybrid protein/solid-state materials. Adv Colloid Interface Sci 270:278–292. https://doi.org/10.1016/j.cis.2019.07.004
7. Yadav B, Chavan S, Atmakuri A, Tyagi RD, Drogui P (2020) A review on recovery of proteins from industrial wastewaters with special emphasis on PHA production process: Sustainable circular bioeconomy process development. Bioresour Technol 317:124006. https://doi.org/10.1016/j.biortech.2020.124006
8. Breathnach AS, Cubbon MD, Karunaharan RN, Pope CF, Planche TD (2012) Multidrug-resistant Pseudomonas aeruginosa outbreaks in two hospitals: association with contaminated hospital

waste-water systems. J Hosp Infect 82:19–24. https://doi.org/10.1016/j.jhin.2012.06.007
9. Lahrich S, Laghrib F, Farahi A, Bakasse M, Saqrane S, El Mhammedi MA (2021) Review on the contamination of wastewater by COVID-19 virus: Impact and treatment. Sci Total Environ 751:1–9. https://doi.org/10.1016/j.scitotenv.2021.142325
10. Vital M, Stucki D, Egli T, Hammes F (2010) Evaluating the growth potential of pathogenic bacteria in water. Appl Environ Microbiol 76:77–84. https://doi.org/10.1128/AEM.00794-10
11. Kurup GG, Adhikari B, Zisu B (2019) Recovery of proteins and lipids from dairy wastewater using food grade sodium lignosulphonate. Water Resour Ind 22:100–114. https://doi.org/10.1016/j.wri.2019.100114
12. Bethi CMS, Narayan B, Martin A, Kudre TG (2020) Recovery, physicochemical and functional characteristics of proteins from different meat processing wastewater streams. Environ Sci Pollut Res 27:25119–25131. https://doi.org/10.1007/s11356-020-08930-x
13. Hwang J, Zhang L, Seo S, Lee YW, Jahng D (2008) Protein recovery from excess sludge for its use as animal feed. Bioresour Technol 99:8949–8954. https://doi.org/10.1016/j.biortech.2008.05.001
14. Li J, Liao X, Zhang Q, Shi B (2013) Adsorption and separation of proteins by collagen fiber adsorbent. J Chromatogr B 928:131–138. https://doi.org/10.1016/j.jchromb.2013.03.031
15. Latour RA (2020) Fundamental principles of the thermodynamics and kinetics of protein adsorption to material surfaces. Colloids Surf B 191:110992. https://doi.org/10.1016/j.colsurfb.2020.110992
16. Bazzaz F, Binaeian E, Heydarinasab A, Ghadi A (2018) Adsorption of BSA onto hexagonal mesoporous silicate loaded by APTES and tannin: isotherm, thermodynamic and kinetic studies. Adv Powder Technol 29:1664–1675. https://doi.org/10.1016/j.apt.2018.04.001
17. Haslam E (2007) Vegetable tannins – Lessons of a phytochemical lifetime. Phytochemistry 68:2713–2721. https://doi.org/10.1016/j.phytochem.2007.09.009
18. Pizzi A (2019) Tannins: prospectives and actual industrial applications. Biomolecules 9:344. https://doi.org/10.3390/biom9080344
19. Arbenz A, Avérous L (2015) Chemical modification of tannins to elaborate aromatic biobased macromolecular architectures. Green Chem 17:2626–2646. https://doi.org/10.1039/C5GC00282F
20. Sartori CJ, Mota GS, Miranda I, Mori FA, Pereira H (2018) Tannin extraction and characterization of polar extracts from the barks of two eucalyptus urophylla hybrids. BioResources 13:4820–4831. https://doi.org/10.15376/biores.13.3.4820-4831
21. Luzardo FHM, Velasco FG, Alves CP, Correia IKS, Cazorla LL (2015) Chemical characterization of agroforestry solid residues aiming its utilization as adsorbents for metals in water. Revi Bras Eng Agric Ambient 19:77–83. https://doi.org/10.1590/1807-1929/agriambi.v19n1p77-83
22. Crestini C, Lange H, Bianchetti G (2016) Detailed chemical composition of condensed tannins via quantitative (31)P NMR and HSQC analyses: *Acacia catechu*, *Schinopsis balansae*, and *Acacia mearnsii*. J Nat Prod 79:2287–2295. https://doi.org/10.1021/acs.jnatprod.6b00380
23. Pizzi A (2021) Covalent and ionic bonding between tannin and collagen in leather making and shrinking: a MALDI-ToF study. J Renew Mater 9:1345–1364. https://doi.org/10.32604/jrm.2021.015663
24. Almeida ON, Menezes RM, Nunes LS, Lemos VA, Luzardo FHM, Velasco FG (2021) Conversion of an invasive plant into a new solid phase for lead preconcentration for analytical purpose. Environ Technol Innov 21:336–346. https://doi.org/10.1016/j.eti.2020.101336
25. Neris JB, Luzardo FHM, Silva EGP, Velasco FG (2019) Evaluation of adsorption processes of metal ions in multi-element aqueous systems by lignocellulosic adsorbents applying different isotherms: a critical review. Chem Eng J 357:404–420. https://doi.org/10.1016/j.cej.2018.09.125
26. Luzardo FHM, Hernández JT, Cazorla LL, Mayworm MAS, Arruda JNDT, Cestari AC (2004) Método químico de inmovilización de taninos en la corteza y su utilización para remover metales pesados de aguas. Oficina Cubana de la Propiedad Industrial. Patent Number: 22929.
27. Sengil A, Özacar M (2009) Competitive biosorption of Pb^{2+}, Cu^{2+} and Zn^{2+} ions from aqueous solutions onto valonia tannin resin. J Hazard Mater 166:1488–1494. https://doi.org/10.1016/j.jhazmat.2008.12.071
28. Luzardo FHM, Velasco FG, Correia IKS, Silva PMS, Salay LC (2017) Removal of lead ions from water using a resin of mimosa tannin and carbon nanotubes. Environ Technol Innov 7:219–228. https://doi.org/10.1016/j.eti.2017.03.002
29. Ghahri S, Pizzi A, Hajihassani R (2022) A study of concept to prepare totally biosourced wood adhesives from only soy protein and tannin. Polymers 14:1150–1160. https://doi.org/10.3390/polym14061150
30. Majorek KA, Porebskia PJ, Dayala A, Zimmermana MD, Jablonskaa K, Stewartd AJ, Chruszcza M, Minor W (2012) Structural and immunologic characterization of bovine, horse, and rabbit serum albumins. Mol Immunol 52:174–182. https://doi.org/10.1016/j.molimm.2012.05.011
31. Hernández EC, Ibirico AM, Cabrera LAM, Luzardo FM, Romero JLS, Borrmann T, Stohrer W-D (2005) Essential amino acids interacting with flavonoids: a theoretical approach. Int J Quantum Chem 103:82–104. https://doi.org/10.1002/qua.20391
32. Koopmann AK, Schuster C, Torres-Rodríguez J, Kain S, Pertl-Obermeyer H, Petutschnigg A, Hüsing N (2020) Tannin-based hybrid materials and their applications: a review. Molecules 25:4910. https://doi.org/10.3390/molecules25214910
33. Thompson M, Ellison SLR, Wood R (2002) Harmonized guidelines for single-laboratory validation of methods of analysis (IUPAC Technical Report). Pure Appl Chem 74:835–855. https://doi.org/10.1351/pac200274050835
34. Grasel FS, Ferrão MF, Wolf CR (2016) Ultraviolet spectroscopy and chemometrics for the identification of vegetable tannins. Ind Crops Prod 91:279–285. https://doi.org/10.1016/j.indcrop.2016.07.022
35. Santos PF, Neris JB, Luzardo FHM, Velasco FG, Tokumoto MS, Cruz RS (2019) Chemical modification of four lignocellulosic materials to improve the Pb^{2+} and Ni^{2+} ions adsorption in aqueous solutions. J Environ Chem Eng 7:1–9. https://doi.org/10.1016/j.jece.2019.103363
36. Marhol M (1982) Ion exchangers in analytical chemistry. their properties and use in inorganic chemistry. Compr Anal Chem 14:81–133. https://doi.org/10.1016/B978-0-444-99717-3.50010-3
37. Verma A, Kumar S, Kumar S (2017) Statistical modeling, equilibrium and kinetic studies of cadmium ions biosorption from aqueous solution using *S. filipendula*. J Environ Chem Eng 5:2290–2304. https://doi.org/10.1016/j.jece.2017.03.044
38. Largitte L, Pasquier R (2016) A review of the kinetics adsorption models and their application to the adsorption of lead by an activated carbon. Chem Eng Res Des 109:495–504. https://doi.org/10.1016/j.cherd.2016.02.006
39. Langmuir I (1916) The constitution and fundamental properties of solids and liquids. J Am Chem Soc 38:2221–2295. https://doi.org/10.1021/ja02268a002
40. Foo KY, Hameed BH (2010) Insights into the modeling of adsorption isotherm systems. Chem Eng J 156:2–10. https://doi.org/10.1016/j.cej.2009.09.013
41. Pizzi A (2003) Natural phenolic adhesives 1: Tannin. In: Pizzi A, Mittal KL (eds). Handbook of Adhesive Technology, pp 573–598.

Marcel Dekker, New York (2003). ISBN: 0-8247-0986-1. https://doi.org/10.1201/9781315120942
42. Correia IKS, Santos PF, Santana CS, Neris JB, Luzardo FHM, Velasco FG (2018) Application of coconut shell, banana peel, spent coffee grounds, eucalyptus bark, piassava (Attalea funifera) and water hyacinth (Eichornia crassipes) in the adsorption of Pb^{2+} and Ni^{2+} ions in water. J Environ Chem Eng 6:2319–2334. https://doi.org/10.1016/j.jece.2018.03.033
43. Kong J, Yu S (2007) Fourier transform infrared spectroscopic analysis of protein secondary structures. Acta Biochim Biophys Sin 39:549–559. https://doi.org/10.1111/j.1745-7270.2007.00320.x
44. Anirudhan TS, Rejeena SR, Tharun AR (2012) Preparation, characterization and adsorption behavior of tannin-modified poly(glycidylmethacrylate)-grafted zirconium oxide-densified cellulose for the selective separation of bovine serum albumin. Colloids Surf B 93:49–58. https://doi.org/10.1016/j.colsurfb.2011.12.010
45. Li H, Liu H, Zhao Q (2020) Adsorption of bovine serum albumin on tannic acid-immobilized chitosan resin. Fibers Polym 21:2440–2447. https://doi.org/10.1007/s12221-020-9667-4
46. Yan J, Zhang QL, Lin DQ, Yao SJ (2014) Protein adsorption behavior and immunoglobulin separation with a mixed-mode resin based on p-aminohippuric acid. J Sep Sci 37:2474–2480. https://doi.org/10.1002/jssc.201400520
47. Shi W, Li M, Jiang C, Shen J, Li K, Zhang S, Zhang J, Han D (2019) Adsorption-selectivity customization and competitive adsorption of tryptamine-based mixed-mode chromatography. Biochem Eng J 150:1–11. https://doi.org/10.1016/j.bej.2019.107267
48. Menkhaus TJ, Fong H (2019) Electrospun nanofibers for protein adsorption. In: Ding B, Wang X, Yu J (eds). Electrospinning: nanofabrication and applications, pp 517–542. Doi:https://doi.org/10.1016/B978-0-323-51270-1.00016-9